



Investigation on the Source of Soil Salinity in Agricultural Land Adjacent to Chamo Lake, Ethiopia

Abenezer Lukas Bassa · Tilahun Kasa ·
Daniel Reddythota · Geleta Tilahun Negatu

Received: 24 January 2023 / Accepted: 27 July 2023 / Published online: 22 August 2023
© The Author(s), under exclusive licence to Springer Nature Switzerland AG 2023

Abstract The soil salinization causing land degradation and decline in soil fertility is becoming a potential problem in some regions of Ethiopia. Finding source of salinization could help devise appropriate measures for solving the problem. The present study was taken up to investigate the source of salinity in an area (1229 ha) lying between the Sile and Elgo rivers near Chamo Lake. The area has remained uncultivated since 2012 and is showing signs of salinity in the form of white deposit on the soil surface. Surface water, groundwater, and soil samples were obtained based on the research area's proximity to potential influencing sources of salinity and fertility decline during the dry and wet seasons. Groundwater samples were taken from seven piezometric stations and eight hand-dug wells while surface water samples were taken from two river sites and four wetland points. The soil samples were taken from four locations. The laboratory results of the groundwater samples in piper diagrams revealed a salt dominance of Ca^{+2} , Mg^{+2} , and Na^{+} with SO_4^{-2} and Cl^{-} . According to the Arc GIS 10.4.1 flow direction analysis tool, the

flow direction of the regional water table towards the lake was northwest to south and southeast. The correlation analysis in Python revealed that Na^{+} and K^{+} , as well as SO_4^{-2} and Cl^{-} , were the most common salt types. Gibbs' theories typically highlighted continuous rock weathering as a significant source of salts in the soils.

Keywords Arenosols · Chamo Lake · Gibbs' plots · Gypsol · Land degradation · Python · Soil salinity

1 Introduction

The land is one of the most essential natural resources since it provides food for humans, animals, and other living things and a means of existence. As a result of salinization, it is vulnerable to deterioration and productivity loss. Over 100 countries have topsoil salinity blowouts, and every continent has salinity (Akoachere et al., 2019). Globally, 950 million ha of land was affected by soil salinity, which is 33% of the world's arable land (Machado & Serralheiro, 2017). Ethiopia is the first country in sub-Saharan Africa where soil salinization has affected 19 million acres of land. In Ethiopia, the soil settings get worse in arid and semi-arid areas due to hostile natural and human-induced factors (Daba & Qureshi, 2021; Savari et al., 2022). About 36% of the total land areas, constituting 44 million ha, were considered saline land. Of this, 33 million ha are dominantly saline, 8 million ha as

A. L. Bassa · T. Kasa · D. Reddythota (✉)
Faculty of Water Supply & Environmental Engineering,
AWTI, Arba Minch University, Arba Minch, Ethiopia
e-mail: daniel.reddy@amu.edu.et; dr.dany77@gmail.com

G. T. Negatu
ArbaMinch Water Technology Institute, Arba Minch
University, Arba Minch, Ethiopia

saline-alkaline, and 3 million ha as dominantly alkaline (Marandia & Shand, 2018).

Soil salinity is currently one of the most pressing issues in the country's arid and semi-arid lowland areas, resulting in lower crop yields, lower farm profits, long-term food insecurity (Artiola et al., 2019), increased rural poverty (Asfaw et al., 2018), and desertification (Daba & Qureshi, 2021). Threshold values (corn — 1.8; banana — 0.4; onion — 1.2; potato — 1.7; tomato — 2.5) are the levels of soil salinity at which plants begin to experience yield-reducing impacts (Newton et al., 1991; Tanji, 1990). Above the threshold, salinity levels are linked with 10, 25, and 50% yield losses (Devkota et al., 2022). Natural causes of soil salinization include climatic, oceanic, topographic, and geological factors, rock weathering (Hassani et al., 2021), rainfall (Mukhopadhyay et al., 2020), raised water table, seawater intrusion in coastal locations (Butcher et al., 2016; Chen et al., 2015), surface evaporation (Cui et al., 2019), plant transpiration (Custodio, 2010), saline groundwater intrusion, and a shallow groundwater table. Human-caused factors include brackish water and saline irrigation water (Liu et al., 2021), inadequate irrigation water management, poor drainage, agricultural chemicals and fertilizers defalcation, and river impoundment (Shokri-Kuehni et al., 2020a, 2020b). The mineral ions Na^+ , Cl^- , Ca^{2+} , SO_4^{-2} , HCO_3^- , K^+ , Mg^{2+} , and NO_3^- were found in soil extracts the majority of the time because of dissolution of minerals and salts in the water (Artiola et al., 2019). Because soil salinization is one of the most serious environmental challenges, it is crucial to analyze soil quality and investigate its harmful repercussions (Ghazaryan & Chen, 2016).

The primary concern in the research area is salinization of agricultural land, which occurs on a regular basis as a result of high salt accumulation, leading to negative impacts on agriculture, and the ecosystem (Daba & Qureshi, 2021). The vicinity has observable white layer coating indicating the presence of salt and thus increases salinity in the area. The source of salinity is unknown and no previous studies undertaken on soil salinization in the area (Ondrasek & Rengel, 2020). The aim of this study was, therefore, to identify the probable cause of the surface soil salinization by analyzing selective parameters in the proximity of water resources and soil of the study area. In this regard, (i) surface water and shallow groundwater

salinity levels were examined at various piezometer locations and private and public boreholes in the research region during the dry and rainy seasons, (ii) groundwater flow direction was determined using Arc GIS, and (iii) the relationship between groundwater and soil surface salinization was assessed using python correlation analysis.

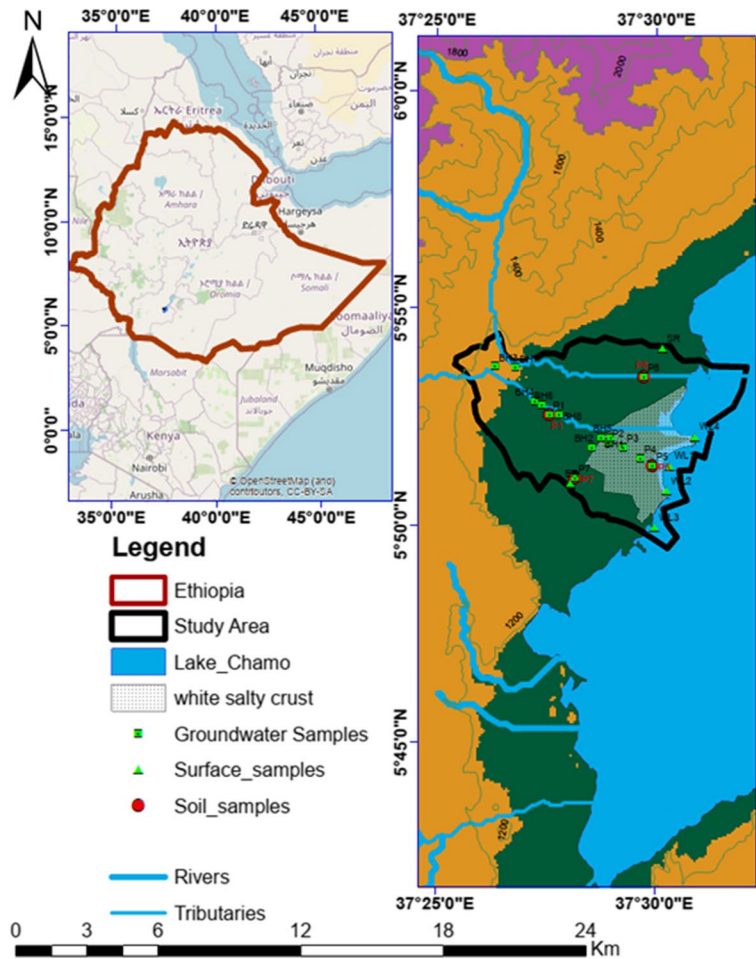
2 Methodology

2.1 Description of Study Area

The research area is located 24 km from the Ethiopian town of Arba Minch, next to the asphalt Arba Minch-Konso road between latitudes of $5^{\circ}48'12''$ and $5^{\circ}54'9''\text{N}$ and longitudes of $37^{\circ}25'9''$ and $37^{\circ}35'50''\text{E}$. Its boundaries are formed by mountains in the north-west and Chamo Lake (329 km^2) in the southeast (Reddythota & Teferi Timotewos, 2022). The research region is traversed by the Sile and Elgo rivers, which empty into Chamo Lake (Fig. 1). The overall research area is 6225.1 ha with a typical furrow irrigation system; agricultural cultivation has ceased over 1229 ha since 2012. The agricultural plains are situated between the Sile and Elgo rivers, with Chamo Lake to its easternmost region. The lake's southwestern part is currently having a salinity problem that has been slowly worsening for many years. The three principal crops grown in the research area are maize, cotton, and bananas. These crops are irrigated by utilizing the neighboring water supplies. The catchment's climate is classified as humid to hot semi-tropical. The catchment's bimodal rainfall pattern consists of two wet seasons (March to mid-June and mid-September to late November) and two dry seasons (December to mid-March and mid-June to mid-September) (FAO, 1994). In the research area, the mean annual temperature and rainfall were 23.9°C and 930 mm, respectively. The evaporation rate is highest during March and July (FAO, 2008).

The area falls under Rift valley which is formed as a result of elevating and faulting action that split a block of the African continent (Foufoula-Georgiou et al., 2015). The Rift valley at Chamo Lake is composed of Quaternary lowland sediments, predominantly of alluvial and lacustrine origin, known as Arenosols (Tarkegn & Jury, 2020). The main components of soil texture were sand, clay, and silt. The

Fig. 1 Location and sampling points of the study area



sediments brought down from the highlands during the pluvial period by the rivers Elgo and Sile as well as other streams have formed the alluvial plains that filled the grabens and stretches of flat ground in the Rift valley (Reddythota & Teferi Timotewos, 2022).

2.2 Sampling and Analysis (Surface Water, Groundwater, and Soil)

Sampling points were selected based on the proximity and prevalence of salinity in the study area. The surface water samples were collected from three water sources, viz., Chamo Lake, Sile River, and Elgo River at six sampling points (Fig. 1). The water samples were collected from Chamo Lake and rivers (Sile and Elgo) were grabbed and time-pace composite (5-min intervals) sampling methods, respectively. The lake samples were garbed from four surrounding

points of the selected sampling point and mixed in a single bucket (space-interval composite samples) then poured into a 1-L sampling bottle. The time-pace discrete samples (5-min intervals) were collected from each selected point from rivers (Fig. 1). The samples were collected and poured into a bucket and mixed, then transferred into 1 L of the appropriately labelled sample container.

Groundwater samples were collected from the seven pre-installed piezometric stations (P1, P2, P3, P4, P5, P7, and P8) located in between the river Sile and Elgo as well as eight bore wells (BH adjacent to the main road, BH next to P2, BH above P2, BH along the main road to Konso, BH close to SR (1), BH close to SR (2), BH next to P1, and BH above P1). Six piezometers were installed perpendicular to the lake and two more were installed parallel to the lake (Fig. 1). The recent flood in Chamo Lake submerged

the piezometric station P6 and was excluded to obtain the water samples. The depth of all the piezometers was similar, i.e., 2 m; however, the water depth varies, and furnished with a plastic pipe which had a cover on the top to protect the intrusion of rainwater and debris from the surroundings. A hosepipe was used to collect the samples from the piezometers. The sediment was allowed to settle before transferring the water sample into the labelled sampling bottle. The collected samples were kept in a cold box to transport to ArbaMinch Water Quality Laboratory for analysis. Electrical conductivity, pH, TDS, SO_4^{-2} , Cl^- , NO_3^- , Na^+ , K^+ , Mg^{2+} , and Ca^{2+} were measured by standard methods (APHA, 2005).

The soil samples were collected from four points in both vertical and horizontal transects close to the surface and groundwater sampling points and white salty crust area. The soil auger was used to collect 300 g of soil samples, from various depths in the range of 0.35–1.87 m until they reach the groundwater table from the surface and put in a labelled polythene sample bag. The soil samples were air-dried at room temperature. The dried soil was ground and sieved through a 2 mm sieve for preparation of the soil paste for further analysis (Gebremeskel et al., 2018). The soil paste was prepared using distilled water in the ratio of 1:5 (Ghazaryan & Chen, 2016). The soil salinity was estimated based on the electrical conductivity of aqueous extracts of soil samples (EC_e) and calculated EC_e by using Equation (1)

$$EC_e = 5.37 * EC_{1.5} + 0.57 \quad (1)$$

The soil texture characterization was done directly in the field by the feel method. This method estimates soil texture qualitatively by “feeling” whether the soil is gritty, coarse, or smooth. Generally, if the moistened soil feels gritty, it is considered as sand, silt if smooth, and clay if sticky.

2.3 Hydrochemical Characteristics of Water

The ionic compositions of water samples were investigated and a kind of water was produced using the AqQA1.5 program. The analytical data were plotted on a piper diagram during both the dry and wet seasons to identify the hydrochemical composition of the water and the type of water. Gibbs diagrams were used intuitively to determine how these

influences affected the primary chemical composition of water (Gibbs, 1970). Gibbs diagrams are a useful tool for identifying the primary natural geochemical processes regulating the hydro-geochemical properties of groundwater in the aquifer (such as precipitation, rock weathering, and evaporation). TDS is plotted against $\text{Na}^+ / (\text{Na}^+ + \text{Ca}^{2+})$ and $\text{Cl}^- / (\text{Cl}^- + \text{HCO}_3^-)$ to produce a Gibbs diagram. The Gibbs diagram used in this study was produced using MS EXCEL 2016.

2.4 Measurement of Water Table Depth of Groundwater

The water table's depth in piezometers and bore wells was measured using a sensor-equipped sound water measuring tape. GPS was used to track the surface elevation of piezometers just above surrounding terrain. At each piezometric station and bore well, the DEM was utilized to determine the ground level in order to precisely compute the water table.

2.5 GIS Application on Groundwater Flow Direction Determination

The flow direction model in Arc GIS was used to determine the direction of regional groundwater flow. The surface elevation of each sampling point from the 30*30 DEM in the study area has been taken into consideration while using the groundwater table data from 15 sites in the study region to spatially interpolate the flow direction. Groundwater occurs in a variety of geological formations and topographic types; these elements frequently regulate the dispersion and extension of the groundwater. In this investigation, programs including Google Earth, Arc GIS, Global Mapper, MS Excel, and Grapher were employed.

2.6 Statistical Analysis of Primary Data

The primary data was analyzed and interpreted by using different computer programs. Statistical analysis was used to justify the accuracy and reliability of the primary data. Descriptive correlation and ANOVA tests were done with SPSS. Descriptive statistics were used for mean computation.

2.6.1 Correlation Analysis of Groundwater Quality and Soil Salinization

The correlation matrix was carried out to assess the relations of physicochemical and biological characteristics of the groundwater, surface water, and soil with its salinity character. The correlation coefficient of Spearman’s rank is expressed by α , the value of which is continuously from -1.0 to $+1.0$. A positive α matches an increasing monotonic trend between two quality parameters, whereas a negative α matches a decreasing monotonic trend among two parameters. A high-level correlation coefficient (nearby -1.0 or 1.0) means an effective relationship between two variables. The value nearby zero means no relationship between the variables (Bennetts et al., 2006). Python software version 2.7.9 was used to plot the correlation matrix.

3 Results and Discussion

3.1 Surface Water Analysis

All examined values in the Sile and Elgo River samples fell within the FAO’s permitted ranges for both the wet and dry seasons, with the exception of electrical conductivity (EC). The EC values in Sile and Elgo river samples during the wet and dry seasons were 0.18 to 0.19 dSm^{-1} and 0.10 to 0.15 dSm^{-1} , respectively (Table 1). EC values in the Chamo Lake

wetland ranged from 0.16 to 11.6 dSm^{-1} and 0.4 to 19.2 dSm^{-1} , respectively, throughout the wet and dry seasons. These values were greater than the allowed limit of 0.03 dSm^{-1} . When compared to river samples, wetlands have greater EC values. The presence of dissolved ions (salts and inorganic) such as sodium, chloride, calcium, and magnesium causes a higher conductivity of electrical current in the water, which indicates increased salinity (Hack et al., 2003). Due to probable factors including dissolved common ions, geology (soil composition), dilution, and land use activities, the higher EC values were found at sampling stations WL1 and WL2 (Daniel, 2008; GSE, 1972).

Potassium concentrations in the wetland sampling points were in the range of 20.2 to 62.5 mg L^{-1} and 8.3 to 37.8 mg L^{-1} during the wet and dry seasons, respectively (Table 1). The entire amount of phosphates and potassium was administered as basal doze during the time of sowing through diammonium phosphate (DAP) and muriate of potash (KCl) fertilizers, respectively. Banana, maize, and onion crops were commonly grown and used 50 to 200 kg ha^{-1} fertilizers (Tadesse et al., 2022). Fertilizers were utilized more than the needed (Sharma et al., 2016). The highest potassium concentration was found at sample site WL1 during the wet season as a result of the input of fertilizers from agricultural fields increasing the nutrient load (Hussain et al., 2006; Sharma et al., 2016). The higher concentration at WL2 site during the dry season may have been due to evaporation.

Table 1 Physicochemical water quality constituents of the surface water samples

Parameters	WHO Stand.	Sile River		Elgo River		Wetlands							
		SR		ER		WL1		WL2		WL3		WL4	
		Wet	Dry	Wet	Dry	Wet	Dry	Wet	Dry	Wet	Dry	Wet	Dry
EC (dSm^{-1})		0.19	0.10	0.18	0.15	19.20	11.20	17.86	11.60	8.80	7.20	0.40	0.16
pH	6.5–8.5	7.70	7.85	7.60	7.50	7.66	7.52	7.90	8.01	7.91	8.00	7.86	7.95
Na^+ (mg/L)	200	47	26.3	43	37.8	1797	1042	1299	844.4	785	643.7	486.2	199.3
K^+ (mg/L)	12	2	1.12	1.5	1.32	62.5	36.3	58.1	37.8	31.5	25.83	20.2	8.3
Mg^{+2} (mg/L)	50	5.82	3.3	4.37	3.9	279	161.8	203.52	132.3	99.01	81.2	26.21	10.7
Ca^{+2} (mg/L)	75	16	8.95	12	10.56	817.6	474.2	561.1	364.7	272.5	223.5	72.1	29.56
Cl^- (mg/L)	250	15	8.4	20	17.6	3784	2195	1491.6	969.6	1011.1	829.2	790.9	324.3
SO_4^{-2} (mg/L)	250	14	7.84	10.5	9.24	714	414.1	490	318.5	238	195.2	63	25.83
NO_3^{-2} (mg/L)	50	2.8	1.56	1.6	1.4	0.4	0.23	0.7	0.45	0.9	0.74	0.81	0.33
TDS (mg/L)	1000	121.6	68.1	115.2	101.4	15360	8909	14288	9287	4008	3287	256	1050

Under conditions of salt stress, it helps to maintain ion homeostasis and regulation of osmotic equilibrium (Hill & Sadowski, 2016). At every sampling point in a wetland, potassium concentrations were higher than authorized limits (2 mg/L).

Magnesium levels at wetland sampling points ranged from 26.21 to 279 mg L⁻¹ and 10.7 to 161.8 mg L⁻¹, respectively, throughout the wet and dry seasons (Table 1). The presence of inorganic nutrients at sampling points WL1, WL2, and WL3 may have caused them to exceed FAO allowable limits (Fiorentini et al., 2021). Calcium and chloride concentrations are higher than the allowable limit in WL1 (during the wet and dry seasons) and WL2 (during the wet season alone). These elevated amounts could be due to inorganic ions and soil texture (Rowley et al., 2018). The elevated chloride concentrations at WL1 and WL2 could possibly be attributed to differences in rock composition and agricultural runoff (Ma et al., 2019).

At the wetland sampling sites, the total dissolved solids ranged from 256 to 15,360 mg L⁻¹ and 1050 to 9287 mg L⁻¹ during the wet and dry seasons, respectively. The sampling stations WL1, WL2, and WL3 were above the allowed limit of 2000 mg L⁻¹, perhaps as a result of changes in agricultural runoff, natural sources, and urban runoff (Mastrocicco & Colombani, 2021). Surface water sampling points WL1 (wet land1) and WL2 had strong saline nature, sampling point WL3 had slightly saline, and sampling points SR (Sele River), ER (Elgo River), and WL4 had non-saline nature as per the results of 12 samples during both seasons.

3.2 Groundwater Analysis

BH1, BH2, and BH6 were dried up during the dry season, making it impossible to collect samples from those locations. During the rainy and dry seasons, respectively, the EC in borehole samples ranged from 0.08 to 20.00 dSm⁻¹ and 0.77 to 23.20 dSm⁻¹, all of which are beyond the permissible limit. As a result, the water had a high salinity, indicating a considerable concentration of common ions (Rodríguez-Rodríguez et al., 2018). At sampling point P5, the EC was maximum during both the wet (20 dSm⁻¹) and dry (23.20 dSm⁻¹) seasons. This result may be related to the types of dissolved ion components due to fertilizers infiltration or soil composition by rock

weathering, and temperature regimes (Hasanuzzaman et al., 2018). The current practice is to apply fertilizer to maize crops at a blanket rate of 100 kg urea and 100 kg diammonium phosphate per ha (64 kg N and 46 kg P₂O₅ ha⁻¹) (Sharma et al., 2016). All ground water sampling points showed greater EC values during the dry season than the wet season, due to different evaporation rates and temperatures.

The sodium levels were between 33.70 and 4572.10 mg L⁻¹ and 18.20 to 6858.80 mg L⁻¹, respectively, throughout the wet and dry seasons. Magnesium levels ranged from 22.60 to 931.2 mg L⁻¹ and 13.5 to 1396.8 mg L⁻¹, respectively, throughout the wet and dry seasons. The range of total dissolved solids (TDS) values during the rainy and dry seasons, respectively, was 51.2 to 16,000.0 mg L⁻¹ and 492.8 to 18,560.0 mg L⁻¹. The sodium, magnesium, and TDS concentrations were above the acceptable limits at sampling points P4 and P5 in both seasons (Figs. 2 and 3). The sodium and magnesium concentration in groundwater will increase as a result of some brines, rocks, and soils containing these minerals dissolving in the water (Mansouri et al., 2022). The elevated values of TDS at sampling points P4 and P5 might be due to carbonate deposits, salt deposits, stormwater, and agricultural runoff (Nachshon, 2016). TDS concentrations raise the water's EC values, which denote increased salinity.

Potassium concentrations were in the range of 0.20 to 11.40 mg L⁻¹ and 1.60 to 1354.70 mg L⁻¹ during the wet and dry seasons, respectively. Potassium concentrations in all sampling points were above the permissible limit of FAO standards, except BH3 (both seasons), BH4 (only wet season), and BH8 (only wet season). The highest concentrations were observed at sampling point P5. These elevated values might be due to leaching of fertilizers (infiltration); brines, igneous and metamorphic rocks or soils, and plant materials in groundwater samplings (Masoud et al., 2022).

Calcium concentrations ranged from 18.2 (BH1) to 520.3 (P5) mg L⁻¹ and 42.7 (BH3) to 926.2 (P5) mg L⁻¹ during the wet and dry seasons, respectively (Figs. 2 and 3). The calcium levels were higher during the dry season than the wet season possibly due to increased evaporation. The highest values were found at sampling point P5, which was the only one that exceeded the permissible limit of 400 mg L⁻¹. These elevated calcium concentrations at sampling point

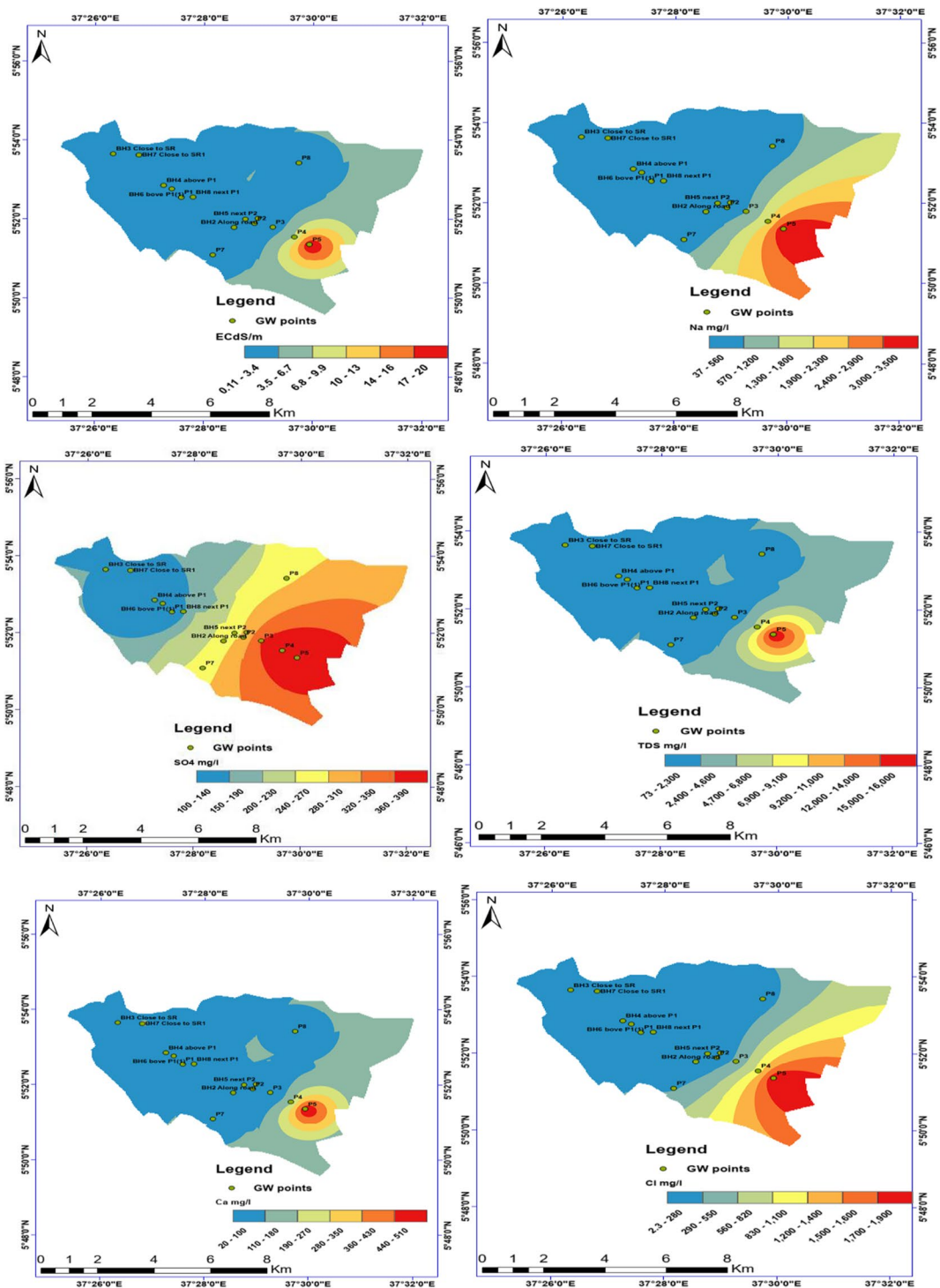


Fig. 2 Ground water quality during the wet season

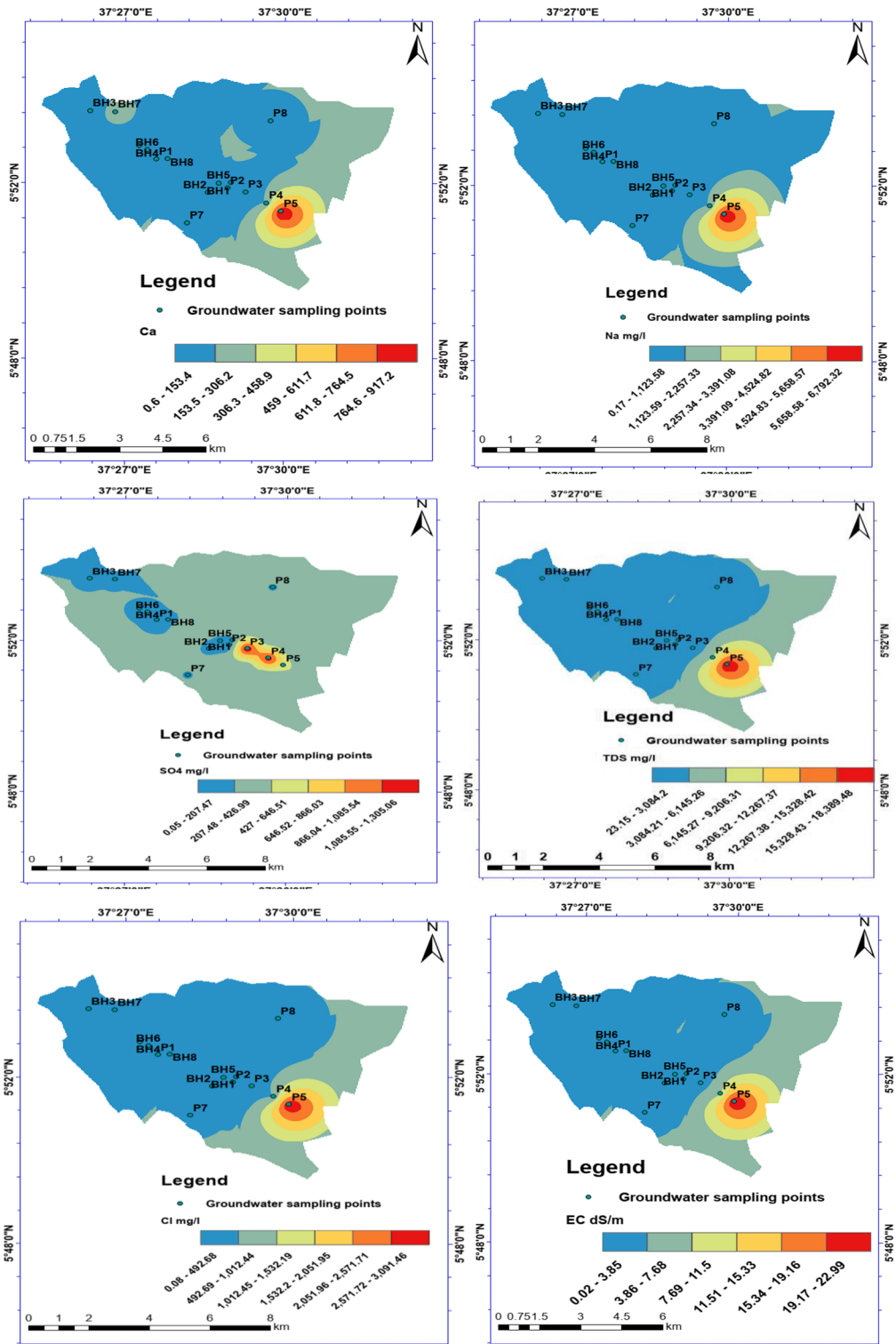


Fig. 3 Ground water quality during the dry season

P5 might be due to the presence of carbonate rocks (limestone and dolomites) in the soil (Qureshi Asad et al., 2019).

Chloride results were in the range of 8.1 (BH4) to 2895.6 (P5) mg L⁻¹ and 15.1 (BH3) to 3121.8 (P5) mg L⁻¹ during the wet and dry seasons, respectively (Figs. 2 and 3). Chloride concentrations were lower in wet seasons, which might be due to the dilution with rainwater (Saha et al., 2019). The highest chloride concentrations were observed at sampling point P5, which might be due to rocks containing chlorides, inorganic fertilizers, and irrigation drainage (Sarath Prasanth et al., 2012).

Sulfate concentrations were in the range of 21.0 (P1) to 994.0 (P3) mg L⁻¹ and 15.8 (P1) to 1322.0 (P3) mg L⁻¹ during the wet and dry seasons, respectively. The concentrations of sulfate in the groundwater were higher than the permissible levels at sampling point P3 during the wet and dry seasons and sampling point P4 during the dry season (Fig. 3). These elevated values of sulfates at P3 and P4 might be due to the presence of carbonate plus gypsum rocks, volcanoes, deposition of fertilizers, and organic matter (Gu & Eastoe, 2021).

Nitrate concentrations in the groundwater sampling points were in the range of 0.05 (BH1, BH3, and BH8) to 14.90 (BH6) mg L⁻¹ and 0.04 (BH8) to 12.20 (BH7) mg L⁻¹ during the wet and dry seasons, respectively (Figs. 2 and 3). The sampling points BH2 and BH6 in the wet season only and sampling point BH7 during both the seasons had above the acceptable limit of nitrates. These elevated nitrate values might be due to the addition of nitrogenous fertilizers (Selemani et al., 2018).

Groundwater sampling points P4 and P5 fell under the category of slightly saline and strongly saline, respectively. Sampling points P2 and P3 fell under the category of very slightly saline during the wet season and non-saline during the dry season, respectively, out of 15 groundwater sampling points in both seasons. All 8 borehole sampling points, P1, P7, and P8 piezometric stations fall under the category of non-saline. The geological and hydro-geological situations (topography, lithology, movement, and depth) play a significant role in the alteration of the groundwater table and water quality (Mebrahtu et al., 2021). These findings revealed that the salinity in the study area was not caused by the Sile or Elgo rivers.

3.3 Soil Analysis

The EC and potassium concentrations in twelve soil samples were in the range of 0.9 to 19.3 dSm⁻¹ and 1.4 to 69.4 dSm⁻¹, respectively (Table 2). All parameters were above the permissible limits at sampling point S2, which might be due to the agricultural runoff water (fertilizers), some brine, igneous and metamorphic rocks, and soil composition (Shahid et al., 2018). Sampling points S1 (20–60 cm and 60–120 cm), S3 (0–20 cm, 20–60 cm, and 60–120 cm), and S4 (0–40 cm, 40–80 cm, and 80–120 cm) fell under the category of “Non-saline”; S1 (0–20 cm), S1 (120–170 cm), and S3 (120–160 cm) fell under the category of “Very slightly saline”; and sampling point S2 fell under the category of “Strongly saline” (Table 3, NRCS Soil Survey handbook). According to these findings, sample points S1, S2, and S3 are unsuitable for the growth of corn, bananas, onions, and potatoes (Devkota et al., 2022; Tanji, 1990).

The soil analysis results showed the highest salinity (strongly saline) at sampling point S2. Small amount of dissolved salts present in the water will be taken by plant roots (Zaman et al., 2018), while the remaining large portion of salt were left in the soil as the water evaporates. As this increases gradually, salinity hazard and toxicity will happen. However, some dissolved salts are crucial for plants (Shil et al., 2019). Sampling points S1 and S3 showed non-saline to slightly saline soil from the second layer to the fourth layer, while sampling point S4 for all the three layers fell under the category of non-saline. The sampling points WL1, WL2, P5, and S2 were the most salty.

4 Discussion

4.1 Groundwater Flow Direction

The groundwater flow channel in the study area was identified by using Arc GIS 10.4.1, 30*30 DEM data, and 15 water level points during the wet season. To make it easier to understand the flow direction, the study area was divided into 31 columns and 23 rows (groundwater flow streaks), and an Arc GIS contour map was created. The flow direction of each cell was monitored to confirm the direction of groundwater

Table 2 The chemical composition of different soil layers in the study area

Sampling point	Depth (cm)	Parameters									
		EC	pH	Na ⁺	K ⁺	Mg ⁺²	Ca ⁺²	Cl ⁻	SO ₄ ⁻²	NO ₃ ⁻	TDS
		dSm ⁻¹		mg L ⁻¹	mg L ⁻¹	mg L ⁻¹	mg L ⁻¹	mg L ⁻¹	mg L ⁻¹	mg L ⁻¹	mg L ⁻¹
FAO Stand.		3	8.5	919	2	60	400	1063	960	10	2000
S1	S1 (0–20)	2.1	7.2	96.6	9.8	9.0	19.3	43.7	5.9	1.8	1331.2
	S1 (20–60)	0.9	7.2	23.2	34.7	16.2	39.5	87.1	11.8	3.6	576.0
	S1 (60–120)	1.7	7.2	74.5	4.5	12.6	37.2	47.9	3.4	1.0	1088.0
S2	S1 (120–170)	4.0	7.3	116.8	10.4	6.4	9.5	20.2	11.8	3.6	2534.4
	S2 (0–30)	19.3	7.1	527.0	69.4	133.3	399.0	700.0	316.4	2.6	14400.0
S3	S3 (0–20)	1.6	7.1	56.0	14.0	3.4	26.6	52.6	3.6	1.1	1024.0
	S3 (20–60)	1.2	7.0	112.0	1.4	3.9	61.9	73.6	4.5	1.4	768.0
	S3 (60–120)	1.4	7.0	191.5	3.6	10.1	0.6	44.8	9.0	2.7	896.0
	S3 (120–160)	2.6	7.4	75.0	5.6	11.2	3.6	145.0	4.8	1.4	1664.0
S4	S4 (0–40)	1.4	7.5	14.0	8.4	1.5	7.3	158.2	0.8	0.3	896.0
	S4 (40–80)	0.9	7.5	5.0	3.9	7.0	11.5	60.2	3.4	1.0	576.0
	S4 (80–120)	1.0	7.9	7.0	4.5	31.9	39.8	77.8	2.8	0.9	640.0

flow (Fig. 4). The flow direction was determined to be greatest from the northwest to the southeast. The groundwater flow direction was determined using the ESRI Direction encoding method and 15 groundwater stations (7 piezometric and 8 water wells). Understanding hydrological processes is critical because they influence salt production in soils and solute transport (Nachshon, 2018). Groundwater recharge and discharge delineation in the watershed aid in determining the salinity deposition area (Jin et al., 2021), water resource use planning, and ecological safety (Loucks & van Beek, 2017). Figure 4 illustrates that the northern and most southwestern parts have relatively steeper contours, indicating that they have a strong potential for groundwater storage and are considered as discharge zones. Figure 4 depicts

the flow direction of groundwater towards the southeastern direction towards the Chamo Lake, which is considered a recharge zone due to gentler slopes.

4.1.1 The Effect of Shallow Groundwater on Soil Salinization

Figure 5 depicts the relationship between groundwater depth and electrical conductivity values of each sampling point. A shallow groundwater table increased electrical conductivity values in the research region, while electrical conductivity is known to decrease with increasing groundwater depth. When the depth exceeds the groundwater table's critical level of 1.2 m, evapotranspiration via vadose seeps through capillarity increases, and salts migrate from deeper strata to the surface (Loucks & van Beek, 2017). The shallow water tables are known to develop saline soils as a result of disproportionate water evaporation, evapotranspiration, and uneven precipitation as well (Ren et al., 2018). Salinity can be rapidly adjusted over time by lateral water flow over a landscape and vertical water fluxes in soils induced by infiltration and evapotranspiration (Boughanmi et al., 2018). Irrigation and rainfall associated with a severe storm can alter the amount and distribution of salts in a soil profile (Tefferia et al., 2019). Reduced water

Table 3 Classes of salinity and EC (1 dSm⁻¹ = 1 mmhoscm⁻¹)

EC (dS/m)	Salinity class
0 < 2	Non-saline
2 < 4	Very slightly saline
4 < 8	Slightly saline
8 < 16	Moderately saline
≥ 16	Strongly saline

Source: NRCS Soil Survey Handbook

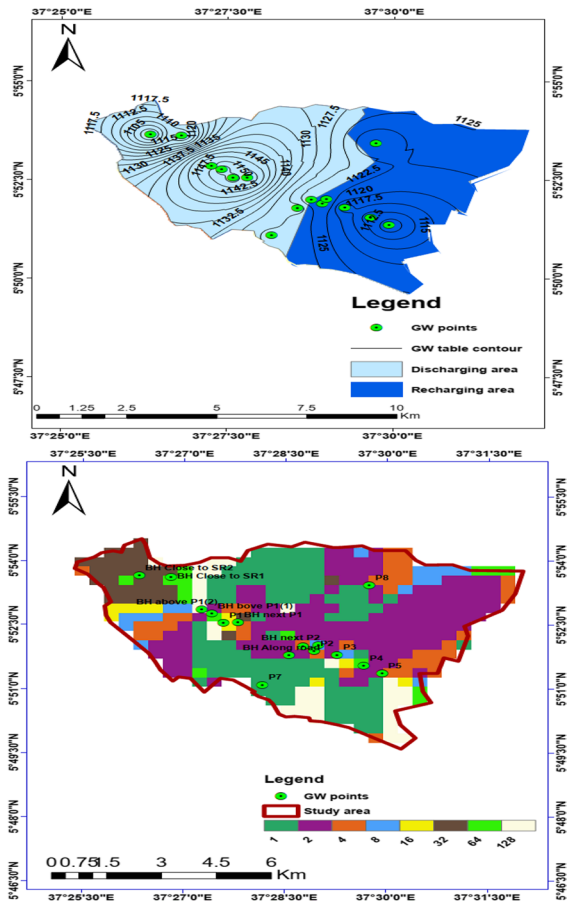
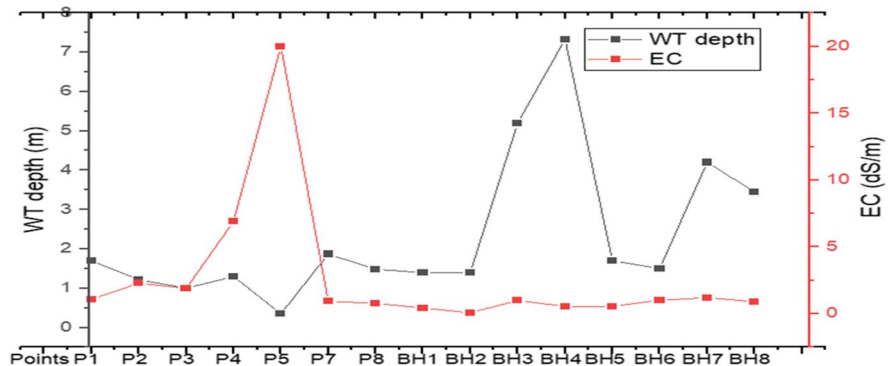


Fig. 4 Groundwater discharge, recharge (a), and flow direction (b)

intake by plants and decreased survival and production are produced by a drop in the osmotic potential between soil pore water and plant root cells, which

Fig. 5 Groundwater depth influence on salinity in terms of EC in the wet season



is induced by an increase in soil pore water solute concentration (Nachshon, 2018).

4.2 Chemical Composition — Salinity — Piper Diagrams

Piper diagrams in the study region allowed for the identification of the potential chemical composition in the groundwater. The very low levels of Ca^{+2} , SO_4^{-2} , and Cl^{-} in the northwest of the research zone may be due to groundwater flowing from the northwest to the southeast (Zaidi et al., 2017). The majority of the Ca^{+2} ions had accumulated at sampling point P5, which may have contributed to the region’s maximum salinity. In the research area, the concentration of Na^{+} ions was relatively similar to the concentration of Ca^{+2} ions (Fig. 6). The SO_4^{-2} is largely deposited in the sampling points P3, P4, and P5, which had concentrations more than 1000 mg L^{-1} . The research area’s SO_4^{-2} and Cl^{-} concentrations may be caused by gypsum deposits, dissolved rock salt, and animal and human waste disposal (Zebire et al., 2019). The findings showed that cations Na^{+} , K^{+} , Mg^{+2} , and Ca^{+2} as well as anions Cl^{-} , SO_4^{-2} , and carbonates were present in the local groundwater during the wet season. The hydrochemistry of the local groundwater also tended to contain carbonates, HCO_3^{-} and SO_4^{-2} , as well as Mg^{+2} , Na^{+} , and K^{+} during the dry season (Fig. 6). In combination, the salt is dominant in Ca^{+2} , Mg^{+2} , and Na^{+} with SO_4^{-2} and Cl^{-} (Fig. 6). High levels of Na^{+} and Cl^{-} entering the soil and groundwater could seriously harm plant growth (Zhang et al., 2021). This could be the cause of the decreased plant growth in the research area.

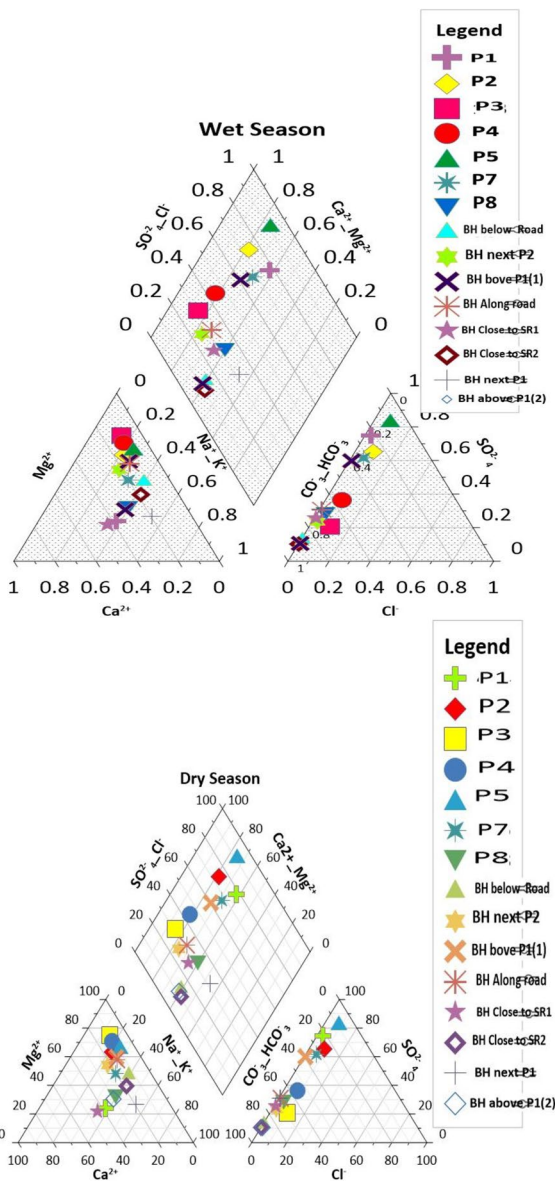


Fig. 6 Piper plots of groundwater hydrochemistry

4.3 Statistical Analysis

Flooding from wetland areas into the study area during the rainy season, according to the researchers' assumptions, could be a cause of salinity (Callow et al., 2020). There was no substantial detection of salt from surface water resources based on study of surface water, wetland, and groundwater samples. The researchers next obtained soil samples at four different depths and observed that sampling points 2

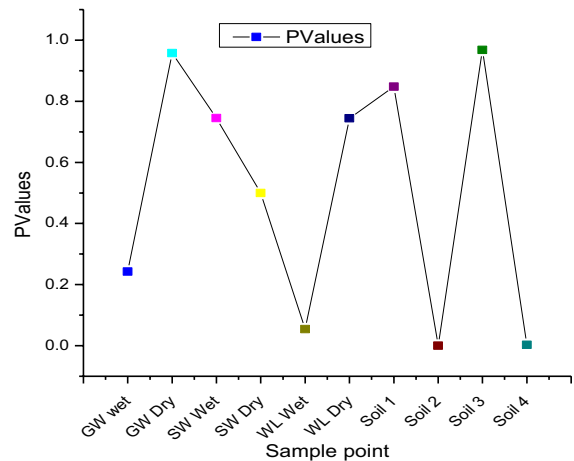


Fig. 7 The results of the analysis of variance

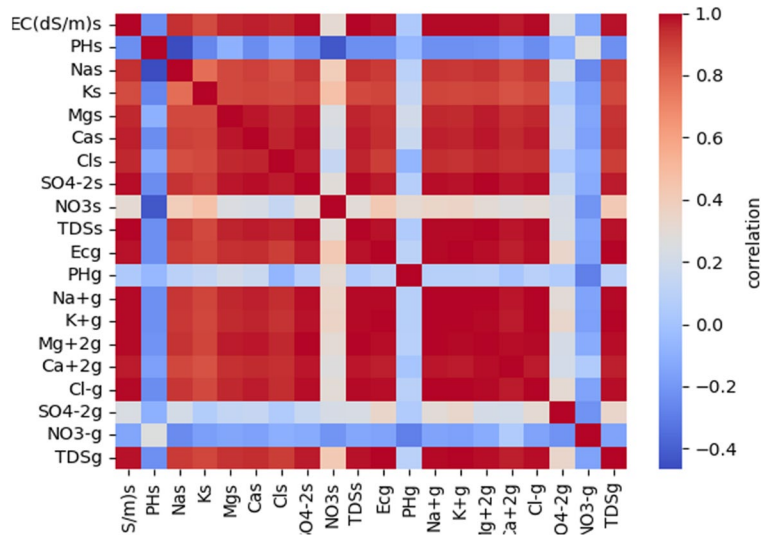
and 4 were particularly significant. The data from the Geological Survey of Ethiopia (GSE, 1972) on the soil profile of the research region was then compared to analytical results, which showed that the salinity was concentrated in the soil's inner layers (Fig. 10) due to carbonate and gypsum. Agricultural activities were discontinued 10 years ago due to a lack of crop growth and production. This could be because previous years' cultivation caused the salt to reach the top strata through the capillary process of plant groundwater usage (Stavi et al., 2021).

The analysis of variance results shown in Fig. 7 revealed that the source of salinity would be from soil because the *P*-value is less than 0.05, which shows "significant." The *P*-values of the surface water (river samples), wetland, and groundwater samples were all greater than 0.05, indicating "no significance."

4.4 The Correlation Relation Between Groundwater and Surface Soil Salinization

The dry season groundwater hydrochemistry and soil quality of the research area were used in the correlation analysis to identify the sources of salinity. The early correlations showed that the pHs and NO₃w have a negative association with the remaining parameters, which are not the source of salinity in the research area (Fig. 8). These correlations described a linear drop in yield as salinity increased (Bennetts et al., 2006; Steppuhn et al., 2005). The ECs and TDSs showed a strong positive association with Na⁺,

Fig. 8 The correlation relation between groundwater and soil chemical composition



Mg²⁺, Ca²⁺, SO₄²⁻, and Cl⁻ in both soil and groundwater, as indicated by the red color in Fig. 8. Especially, EC of the soil showed a very strong relation to the soil SO₄²⁻s and groundwater parameters of ECw, Na⁺w, K⁺w, Mg²⁺w, and TDSw (Fig. 8). This correlation result clearly showed the southeastern area's salinity due to salty groundwater flow from the strongly saline zone (Thien, 1979). With the exception of pHs and NO₃w, the remaining all ions displayed positive associations with one another, implying that the saline zone may be their likely source from the soil texture (Gypsol).

4.5 Gibbs Diagrams — Sources of Salinity

The Gibbs diagrams reveal the relationship between anions [Cl/(Cl+SO₄)] and cations [Na/(Na+Ca)] and TDS in the groundwater samples (Tuladhar & Iqbal, 2020; Vessia & Russo, 2017). These anions and cations relationships help to identify the sources of dissolved chemical constituents in the groundwater, such as precipitation, geology, and evaporation. The greatest EC values were recorded at sampling points WL1, WL2, P5, and S2 and were 19.20, 17.86, 20.00, and 19.3 dSm⁻¹ in the wet season and 11.2, 11.6, 23.2, and 19.3 dSm⁻¹ in the dry season, respectively. To confirm the origins of salinity in the research area, Gibbs plots were created (Fig. 9).

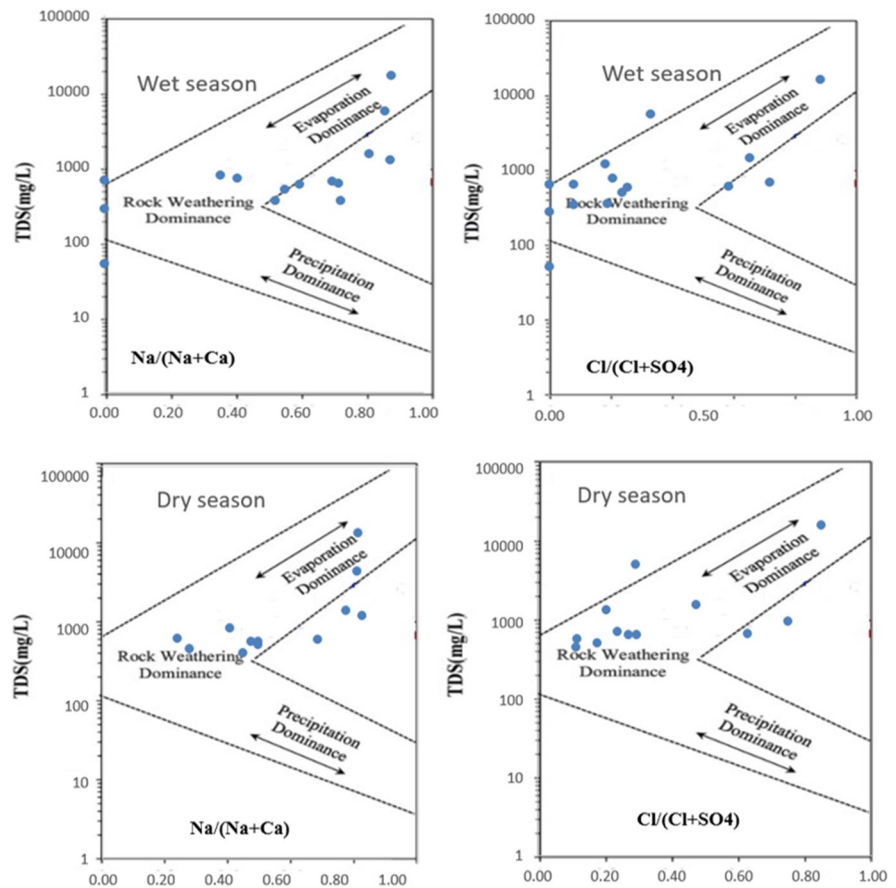
The Gibbs diagram is frequently used to determine the relationship between water composition and aquifer lithological features (Wang & Shan, 2015).

The Gibbs diagram indicated groundwater soil and aquifer parameters on the left and right, respectively. The lower Na/(Na+Ca) ratio indicates that carbonates predominate in the examined area (Chenchen et al., 2019). The Gibbs diagram depicts four separate fields: precipitation dominance, evaporation dominance, rock weathering dominance, and human-induced dominance. According to the findings, all of the primary cations are from rock-weather dominance and human-induced dominance during the wet season (Feng et al., 2020). In the dry season, however, most cations were obtained by the dominance of rock-weathering and evaporation, with just a small amount obtained through human-induced dominance. These Gibbs plots revealed rock-weather dominance as the primary cause of salinity (Fig. 9). The soil texture map of the research area revealed the presence of alluvial lacustrine deposits with carbonate and gypsum salts known as Gypsol (Yu et al., 2020). These Gibbs plots confirmed that salinity was caused by rock-weathering, which suggests Arenosols soil texture. During the dry season due to evaporation as well as maize, cotton and banana cultivation salinity might be reaching the upper layers of the soil.

5 Conclusion

The sampling locations WL1 (19.2), WL2 (17.8), P5 (20.00), and S2 (19.3) were all significantly saline. The presence of Na⁺, K⁺, Cl⁻, and SO₄²⁻ ions in

Fig. 9 Gibbs plot of groundwater hydrochemistry in the wet and dry seasons



the research area contributed to the saline character, which was also supported by the correlation analysis. The geochemical combination of Na^+ , Cl^- , and SO_4^{2-} would be the reason for the salinity that inhibited plant development in the studied region. The causes of salinity in the study area were rock weathering, evaporation, and little human influence, as corroborated by Gibbs' plots. This study concluded that the salinity in the studied area was caused by the soil composition of Arenosols, agricultural operations, and input of fertilizers, rather than by surface water or groundwater. The study area soil is not suitable for corn, banana, potatoes, and onion for cultivation. Finally, geological formations caused land deterioration in the studied area.

Acknowledgements The authors are grateful to the Faculty of Water Supply & Environmental Engineering, AWTI, Arba Minch University, Ethiopia, for providing laboratory and instruments support to conduct this research work successfully.

Author Contribution ALB: conducting a research and investigation process, specifically performing the experiments, or data/evidence collection, collection, analysis of the samples, field work, survey, data collection, Arc GIS mapping.

TK: data curation, statistical analysis of data, review, and editing, Arc GIS mapping.

DR: conceptualization, plan of research work, methodology, data curation, writing—original draft preparation, review and editing, supervision.

GT: data curation, Arc GIS mapping, data collection, review and editing.

Data Availability The datasets used and/or analyzed during the current study are available from the corresponding author on reasonable request.

Declarations

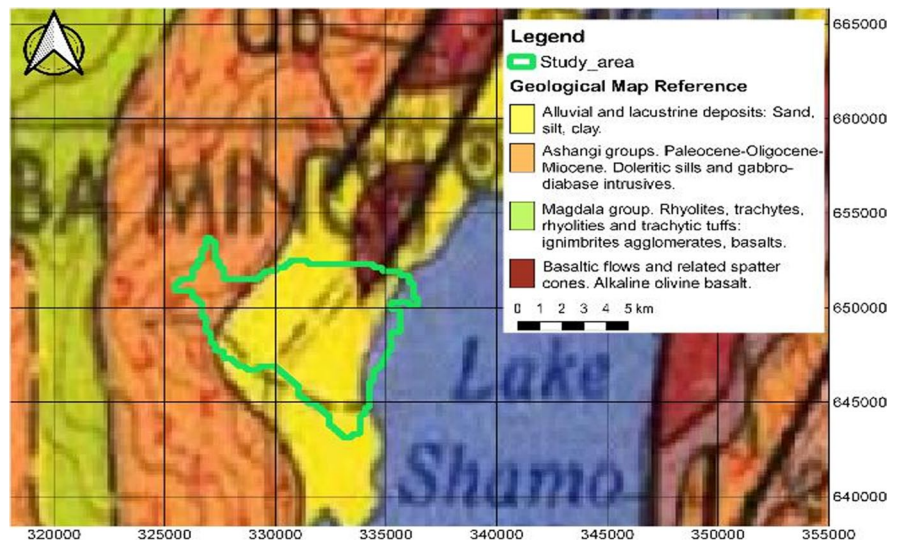
Ethics Approval and Consent to Participate Not applicable.

Consent for Publication Not applicable.

Competing Interests The authors declare no competing interests.

Appendix

Fig. 10 Geological composition in the study area (source: Geological Survey of Ethiopia, 1972)



References

- Akoachere, R. A., Yaya, O. O., Egbe, S. E., Eyang, T. A., Nji, B. N., & Tambe, D. B. (2019). GIS-hydrogeochemical model of the Yaoundé Fractured Rock Aquifer, Cameroon: Aquifer setting, seasonal variations in groundwater-rock interaction and water quality. *Journal of Geoscience and Environment Protection*, 7, 232–263.
- APHA. (2005). *Standard methods for the examination of water and waste water* (21st ed.). American Public Health Association.
- Artiola, J. F., Walworth, J. L., Musil, S. A., & Crimmins, M. A. (2019). *Soil and land pollution*. In *Environmental and Pollution Science* (3rd ed.). Elsevier Inc. <https://doi.org/10.1016/b978-0-12-814719-1.00014-8>
- Asfaw, E., Suryabhadgavan, K. V., & Argaw, M. (2018). Soil salinity modelling and mapping using remote sensing and GIS: The case of Wonji sugar cane irrigation farm, Ethiopia. *Journal of the Saudi Society of Agricultural Sciences*, 17(3), 250–258. <https://doi.org/10.1016/j.jssas.2016.05.003>
- Bennetts, D. A., Webb, J. A., Stone, D. J. M., & Hill, D. M. (2006). Understanding the salinization process for groundwater in an area of south-eastern Australia, using hydrochemical and isotopic evidence. *Journal of Hydrology*, 323(1–4), 178–192.
- Boughanmi, M., Dridi, L., Hamdi, M., Majdoub, R., & Schäfer, G. (2018). Impact of floodwaters on vertical water fluxes in the deep vadose zone of an alluvial aquifer in a semi-arid region. *Hydrological Sciences Journal*, 63(1), 136–153. <https://doi.org/10.1080/02626667.2017.1410281>
- Butcher, K., Wick, A. F., DeSutter, T., Chatterjee, A., & Harmon, J. (2016). Soil salinity: A threat to global food security. *Agronomy Journal*, 108, 2189–2200.
- Callow, J. N., Hipsey, M. R., & Vogwill, R. I. J. (2020). Surface water as a cause of land degradation from dryland salinity. *Hydrology and Earth System Sciences*, 24, 717–734. <https://doi.org/10.5194/hess-24-717-2020>
- Chen, Y., Li, W., Xu, C., Ye, Z., & Chen, Y. (2015). Desert riparian vegetation and groundwater in the lower reaches of the Tarim river basin. *Environmental Earth Sciences*, 73, 547–558.
- Chenchen, W., Li, F., Yang, P., Ren, S., Wang, S., Yu, W., Ziang, X., Yao, X., Wei, R., & Zhang, Y. (2019). Effects of irrigation water salinity on soil properties, N₂O emission and yield of spring maize under mulched drip irrigation. *Water*, 11, 1548. <https://doi.org/10.3390/w11081548>
- Cui, G., Lu, Y., Zheng, C., Liu, Z., & Sai, J. (2019). Relationship between soil salinization and groundwater hydration in Yaoba Oasis, Northwest China. *Water (Switzerland)*, 11(1). <https://doi.org/10.3390/w11010175>
- Custodio, E. (2010). Coastal aquifers of Europe: An overview. *Hydrogeology Journal*, 18, 269–280.
- Daba, A. W., & Qureshi, A. S. (2021). Review of soil salinity and sodicity challenges to crop production in the lowland irrigated areas of Ethiopia and its management strategies. *Land*, 10(12), 1377. <https://doi.org/10.3390/land10121377>
- Daniel, H. (2008). *Soil fertility and plant nutrition — Soil in the environment*. Elsevier Publishers. <https://doi.org/10.1016/C2009-0-00041-5>
- Devkota, K. P., Devkota, M., Rezaei, M., & Oosterbaan, R. (2022). Managing salinity for sustainable agricultural production in salt-affected soils of irrigated dry lands. *Agricultural Systems*, 198, 103390. <https://doi.org/10.1016/j.agry.2022.103390>
- FAO. (1994). *Water quality for agriculture, irrigation and drainage*. Food and Agriculture Organization of the United Nations.

- FAO, Motsara, M. R., & Roy, R. N. (2008). *Guide to laboratory establishment for plant nutrient analysis*. Food and Agriculture Organization of the United Nations.
- Feng, W., Qian, H., Panpan, X., & Hou, K. (2020). Hydrochemical characteristic of groundwater and its impact on crop yields in the Baojixia irrigation area, China. *Water*, *12*, 1443. <https://doi.org/10.3390/w12051443>
- Fiorentini, D., Cappadone, C., Farruggia, G., & Prata, C. (2021). Magnesium: Biochemistry, nutrition, detection, and social impact of diseases linked to its deficiency. *Nutrients*, *13*, 1136. <https://doi.org/10.3390/nu13041136>
- Foufoula-Georgiou, E., Takbiri, Z., Czuba, J. A., & Schwenk, J. (2015). The change of nature and the nature of change in agricultural landscapes: Hydrologic regime shifts modulate ecological transitions. *Water Resources Research*, *51*, 6649–6671.
- Gebremeskel, G., Gebremicael, T. G., Kifle, M., Meresa, E., Gebremedhin, T., & Girmay, A. (2018). Salinization pattern and its spatial distribution in the irrigated agriculture of Northern Ethiopia: An integrated approach of quantitative and spatial analysis. *Agricultural Water Management*, *206*, 147–157. <https://doi.org/10.1016/j.agwat.2018.05.007>
- Geological Survey of Ethiopia (GSE) (1972). ArbaMinch Zuria geological pattern.
- Ghazaryan, K., & Chen, Y. (2016). Hydrochemical assessment of surface water for irrigation purposes and its influence on soil salinity in Tikanlik oasis, China. *Environmental Earth Sciences*, *75*(5), 1–15. <https://doi.org/10.1007/s12665-016-5287-0>
- Gibbs, R. J. (1970). Mechanisms controlling world water chemistry. *Science*, *170*, 1088–1090.
- Gu, A., & Eastoe, C. J. (2021). The origins of sulfate in Cenozoic non-marine evaporites in the basin and-range province, Southwestern North America. *Geosciences*, *11*, 455. <https://doi.org/10.3390/geosciences11110455>
- Hack, R., Price, D., & Rengers, N. (2003). A new approach to rock slope stability — A probability classification (SSPC). *Bulletin of Engineering Geology and the Environment*, *62*, 167–184. <https://doi.org/10.1007/s10064-002-0155-4>
- Hasanuzzaman, M., Bhuyan, M. H. M. B., Nahar, K., Hossain, M. S., Al Mahmud, J., Hossen, M. S., Masud, A. A. C., Moumita, & Fujita, M. (2018). Potassium: A vital regulator of plant responses and tolerance to abiotic stresses. *Agronomy*, *8*, 31. <https://doi.org/10.3390/agronomy8030031>
- Hassani, A., Azapagic, A., & Shokri, N. (2021). Global predictions of primary soil salinization under changing climate in the 21st century. *Nature Communications*, *12*, 6663. <https://doi.org/10.1038/s41467-021-26907-3>
- Hill, A. R., & Sadowski, E. K. (2016). Chloride concentrations in wetlands along a rural to urban land use gradient. *Wetlands*, *36*, 73–83. <https://doi.org/10.1007/s13157-015-0717-4>
- Hussain, N., Ali Ai-Rawahy, S., Rabee, J., & Ai-Amri, M. (2006). Causes, origin, genesis and extent of soil salinity in the sultanate of Oman. *The Journal of Agricultural Science*, *43*, 1–2.
- Jin, L., Whitehead, P. G., Bussi, G., Hirpa, F., Taye, M. T., Abebe, Y., & Charles, K. (2021). Natural and anthropogenic sources of salinity in the Awash River and Lake Beseka (Ethiopia): Modelling impacts of climate change and lake-river interactions. *Journal of Hydrology: Regional Studies*, *36*, 100865. <https://doi.org/10.1016/j.ejrh.2021.100865>
- Liu, C., Cui, B., Chao, H., Haiqing, W., & Gao, F. (2021). Effects of mixed irrigation using brackish water with different salinities and reclaimed water on a soil-crop system. *Journal of Water Reuse and Desalination*, *11*(4), 632–648. <https://doi.org/10.2166/wrd.2021.043>
- Loucks, D. P., & van Beek, E. (2017). Water resources planning and management: An overview. In *Water Resource Systems Planning and Management*. Springer. https://doi.org/10.1007/978-3-319-44234-1_1
- Ma, L., Wang, X., Gao, Z., Youke, W., Nie, Z., & Liu, X. (2019). Canopy pruning as a strategy for saving water in a dry land jujube plantation in a loess hilly region of China. *Agricultural Water Management*, *216*, 436–443.
- Machado, R. M. A., & Serralheiro, R. P. (2017). Soil salinity: Effect on vegetable crop growth. Management Practices to Prevent and Mitigate Soil Salinization. *Horticulturae*, *3*, 30. <https://doi.org/10.3390/horticulturae3020030>
- Mansouri, Z., Leghrieb, Y., Kouadri, S., Al-Ansari, N., Najm, H. M., Mashaan, N. S., Eldirderi, M. M. A., & Khedher, K. M. (2022). Hydro-geochemistry and groundwater quality assessment of Ouargla Basin, South of Algeria. *Water*, *14*, 2441. <https://doi.org/10.3390/w14152441>
- Marandia, A., & Shand, P. (2018). Groundwater chemistry and the Gibbs diagram. *Applied Geochemistry*, *97*, 2009–2012. <https://doi.org/10.1016/j.apgeochem.2018.07.009>
- Masoud, M., El Osta, M., Alqarawy, A., et al. (2022). Evaluation of groundwater quality for agricultural under different conditions using water quality indices, partial least squares regression models, and GIS approaches. *Applied Water Science*, *12*, 244. <https://doi.org/10.1007/s13201-022-01770-9>
- Mastrociccio, M., & Colombani, N. (2021). The issue of groundwater salinization in coastal areas of the Mediterranean region: A review. *Water*, *13*, 90. <https://doi.org/10.3390/w13010090>
- Mebrahtu, T. K., Banning, A., Girmay, E. H., et al. (2021). The effect of hydrogeological and hydrochemical dynamics on landslide triggering in the central highlands of Ethiopia. *Hydrogeology Journal*, *29*, 1239–1260. <https://doi.org/10.1007/s10040-020-02288-7>
- Mukhopadhyay, R., Sarkar, B., Jat, H. S., Sharma, P. C., & Bolan, N. S. (2020). Soil salinity under climate change: Challenges for sustainable agriculture and food security. *Journal of Environmental Management*, *280*, 111736.
- Nachshon, U. (2016). Seepage weathering impacts on erosivity of arid stream banks: A new conceptual model. *Geomorphology*, *261*, 212–221.

- Nachshon, U. (2018). Cropland soil salinization and associated hydrology: Trends, processes and examples. *Water*, 10, 1030. <https://doi.org/10.3390/w10081030>
- Newton, P. J., Myers, B. A., & West, D. W. (1991). Reduction in growth and yield of Jerusalem artichoke caused by soil salinity. *Irrigation Science*, 12, 213–221.
- Ondrasek, G., & Rengel, Z. (2020). Environmental salinisation processes: Detection, implications & solutions. *Science of the Total Environment*, 754, 142432.
- Qureshi Asad, S., Mohammed, M., Daba, A. W., Hailu, B., Belay, G., Tesfaye, A., & Ertebo, T. M. (2019). Improving agricultural productivity on salt-affected soils in Ethiopia: Farmers' perceptions and proposals. *African Journal of Agricultural Research*, 14(21), 897–906. <https://doi.org/10.5897/AJAR2019.14077>
- Reddythota, D., & Teferi Timotewos, M. (2022). Evaluation of pollution status and detection of the reason for the death of fish in Chamo Lake, Ethiopia. *Journal of Environmental and Public Health*, 2022, 5859132. <https://doi.org/10.1155/2022/5859132>
- Ren, D., Xu, X., Huang, Q., Huo, Z., Xiong, Y., & Huang, G. (2018). Analyzing the role of shallow groundwater systems in the water use of different land-use types in arid irrigated regions. *Water*, 10(5), 634. <https://doi.org/10.3390/w10050634>
- Rodríguez-Rodríguez, M., Fernández-Ayuso, A., Hayashi, M., & Moral-Martos, F. (2018). Using water temperature, electrical conductivity, and pH to characterize surface-groundwater relations in a shallow ponds system (Doñana National Park, SW Spain). *Water*, 10, 1406. <https://doi.org/10.3390/w10101406>
- Rowley, M. C., Grand, S., & Verrecchia, É. P. (2018). Calcium-mediated stabilisation of soil organic carbon. *Biogeochemistry*, 137, 27–49. <https://doi.org/10.1007/s10533-017-0410-1>
- Saha, S., Reza, A. H. M. S., & Roy, M. K. (2019). Hydro chemical evaluation of groundwater quality of the Tista floodplain, Rangpur, Bangladesh. *Applied Water Science*, 9, 198.
- Sarath Prasanth, S. V., Magesh, N. S., & Jitheshlal, K. V. (2012). Evaluation of groundwater quality and its suitability for drinking and agricultural use in the coastal stretch of Alappuzha District, Kerala, India. *Applied Water Science*, 2, 165–175. <https://doi.org/10.1007/s13201-012-0042-5>
- Savari, M., Yazdanpanah, M., & Rouzaneh, D. (2022). Factors affecting the implementation of soil conservation practices among Iranian farmers. *Scientific Reports*, 12, 8396. <https://doi.org/10.1038/s41598-022-12541-6>
- Selemani, J., Zhang, J., Muzuka, A., Njau, K. N., Zhang, G., Mzusa, M., & Maggid, A. (2018). Nutrients' distribution and their impact on Pangani River Basin's ecosystem-Tanzania. *Environmental Technology*, 39, 702–716.
- Shahid, S. A., Zaman, M., & Heng, L. (2018). Soil salinity: Historical perspectives and a world overview of the problem. In *Guideline for Salinity Assessment, Mitigation and Adaptation Using Nuclear and Related Techniques*. Springer. https://doi.org/10.1007/978-3-319-96190-3_2
- Sharma, P. D., Adare, K., Girma, A., & Lemma, B. (2016). Response of maize to fertilization on alluvial soil in Arba-Minch, Gamo-Gofa, Southern Ethiopia. *International Journal of Agricultural Sciences*, 6(9), 1141–1147.
- Shil, S., Singh, U. K., & Mehta, P. (2019). Water quality assessment of a tropical river using water quality index (WQI), multivariate statistical techniques and GIS. *Applied Water Science*, 9(7), 1–21. <https://doi.org/10.1007/s13201-019-1045-2>
- Shokri-Kuehni, S. M. S., Raaijmakers, B., Kurz, T., Or, D., Helmig, R., & Shokri, N. (2020b). Water table depth and soil salinization: From pore-scale processes to field-scale responses. *Water Resources Research*, 56, e2019WR026707. <https://doi.org/10.1029/2019WR026707> Received 6 NOV 2019 Accepted 17 JAN 2020 Accepted article online 20 JAN 2020 SHOKRI-KUEHNI ET AL.1of13.
- Shokri-Kuehni, S. M. S., Raaijmakers, B., Kurz, T., Or, D., Helmig, R., & Shokri, N. (2020a). Water table depth and soil salinization: From pore-scale processes to field-scale responses. *Water Resources Research*, 56(2), e2019WR026707. <https://doi.org/10.1029/2019WR026707>
- Stavi, I., Thevs, N., & Priori, S. (2021). Soil salinity and sodicity in drylands: A review of causes, effects, monitoring, and restoration measures. *Frontiers in Environmental Science*, 9, 712831. <https://doi.org/10.3389/fenvs.2021.712831>
- Stappuhn, H., Van Genuchten, M. T., & Grieve, C. M. (2005). Root-zone salinity: I. Selecting a product-yield index and response function for crop tolerance. *Crop Science*, 45, 209–220.
- Tadesse, T., Sharma, P. D., & Ayele, T. (2022). Effect of the irrigation interval and nitrogen rate on yield and yield components of onion (*Allium cepa* L.) at Arba Minch, Southern Ethiopia. *Advances in Agriculture*, 2022, 4655590. <https://doi.org/10.1155/2022/4655590>
- Tanji. (1990). In K. K. Tanji (Ed.), *Agricultural salinity assessment and management*. 1990. American Society of Civil Engineers.
- Tarkegn, G. B., & Jury, M. R. (2020). Changes in the seasonality of Ethiopian highlands climate and implications for crop growth. *Atmosphere*, 11, 892. <https://doi.org/10.3390/atmos11090892>
- Teffera, F. E., Lemmens, P., Deriemaeker, A., Deckers, J., Bauer, H., Gamo, F. W., Brendonck, L., & Meester, L. D. (2019). Why are Lake Abaya and Lake Chamo so different? A limnological comparison of two neighboring major Ethiopian Rift Valley lakes. *Hydrobiologia*, 829, 113–124. <https://doi.org/10.1007/s10750-018-3707-8>
- Thien, S. J. (1979). A flow diagram for teaching texture-by-feel analysis. *Journal of Agronomic Education*, 8(1), 54–55.
- Tuladhar, S., & Iqbal, M. (2020). Investigating the critical role of a wetland in spatial and temporal reduction of

- environmental contaminants: A case study from Iowa, USA. *Wetlands*, 40, 101–112. <https://doi.org/10.1007/s13157-019-01162-x>
- Vessia, G., & Russo, S. (2017). Classification of lacustrine sediments based on sedimentary components. *Biosystems Engineering*, 168, 4–13. <https://doi.org/10.1016/j.biosystemseng.2017.08.023>
- Wang, Q. J., & Shan, Y. Y. (2015). Review of research development on water and soil regulation with brackish water irrigation. *Transactions of the Chinese Society of Agricultural Machinery*, 46, 117–126.
- Yu, G., Wang, J., & Liu, L. (2020). The analysis of groundwater nitrate pollution and health risk assessment in rural areas of Yantai, China. *BMC Public Health*, 20, 437. <https://doi.org/10.1186/s12889-020-08583-y>
- Zaidi, F. K., Al-Bassam, A. M., Kassem, O. M. K., Alfaihi, H. J., & Alhumidan, S. M. (2017). Factors influencing the major ion chemistry in the Tihama coastal plain of southern Saudi Arabia: Evidences from hydrochemical facies analyses and ionic relationships. *Environmental Earth Sciences*, 76, 472.
- Zaman, M., Shahid, S. A., & Heng, L. (2018). Irrigation water quality. In *Guideline for Salinity Assessment, Mitigation and Adaptation Using Nuclear and Related Techniques*. Springer. https://doi.org/10.1007/978-3-319-96190-3_5
- Zebire, D. A., Ayele, T., & Ayana, M. (2019). Characterizing soils and the enduring nature of land uses around the Lake Chamo Basin in South-West Ethiopia. *Journal of Ecology and Environment*, 43(1), 1–32. <https://doi.org/10.1186/s41610-019-0104-9>
- Zhang, S., Wei, J., Li, Y., Duan, M., Nwankwegu, A. S., & Norgbey, E. (2021). The influence of seasonal water level fluctuations on the soil nutrients in a typical wetland reserve in Poyang Lake, China. *Sustainability*, 13, 3846. <https://doi.org/10.3390/su13073846>

Publisher's Note Springer Nature remains neutral with regard to jurisdictional claims in published maps and institutional affiliations.

Springer Nature or its licensor (e.g. a society or other partner) holds exclusive rights to this article under a publishing agreement with the author(s) or other rightsholder(s); author self-archiving of the accepted manuscript version of this article is solely governed by the terms of such publishing agreement and applicable law.